Chemical genetic approaches for target validation

Wel, T. van der

4

Covalent complementary probes reveal the role of FES tyrosine kinase in neutrophil phagocytosis via SYK activation

Introduction

Neutrophils are the most abundant members of the innate immune system, which serve as the first line of host defense against invading pathogens and respond immediately upon infection.[1] They are recruited to the site of infection and their primary function is to internalize and eliminate the pathogen via a process named phagocytosis. The first step in phagocytosis is recognition of the pathogen, which can occur via (a cross-talk of) various immunoreceptors, including pathogen-associated molecular pattern (PAMP) receptors, Fc-gamma receptors (FcγRs) and complement receptors (CRs).[2] Each immunoreceptor subsequently activates an internalization machinery, ultimately leading to phagosome formation, maturation, and killing of the pathogen. Neutrophils possess a wide range of mechanisms to kill pathogens, including the production of reaction oxygen species (ROS), release of cytotoxic granule components and antimicrobial peptides, and formation of neutrophil extracellular traps (NETs).[3] Elucidation of the molecular components of the phagocytic pathway is of importance to design novel anti-infective agents and molecular therapies for autoimmune disorders.

The non-receptor tyrosine kinase FES is highly expressed in phagocytes, where it is activated upon stimulation of various pathogen-recognizing receptors, including Toll-like receptor 4 (TLR4) by lipopolysaccharide (LPS) in macrophages[4,5] and high-affinity immunoglobulin E receptor I (FcεRI) by IgE in mast cells.[6] FES is located in signaling pathways linked to regulation of the actin cytoskeleton, cell migration and the release of inflammatory mediators. However, the role of FES and its downstream substrates in neutrophils has not been investigated so far.

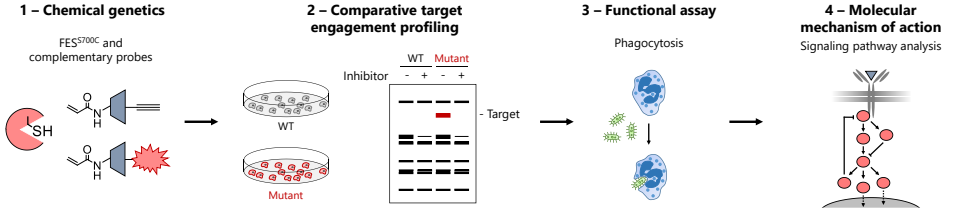

Figure 4.1 – Chemical genetics workflow to study the role of FES in neutrophil phagocytosis. Schematic workflow encompassing the application of chemical genetic tools and endogenous model system described in chapters 2 and 3. Comparative profiling using wild-type and FES^{S700C} HL-60 cells can be used to visualize target engagement of FES upon *in situ* treatment with WEL028. Phagocytosis can subsequently be measured in a flow cytometry-based assay using fluorescent bacteria. Analysis of associated signaling pathways, *e.g.* by phospho-specific immunoblot analysis, provides insight in the molecular mechanism of action of the target kinase.

Here, the role of FES in phagocytosis of live bacteria by neutrophils was studied. The chemical genetic toolbox described in chapter 2 (Figure 4.1, step 1) is suited to selectively inactivate endogenous FES^{S700C} in the generated mutant HL-60 cell line (Figure 4.1, step 2). Comparative target engagement profiling led to the discovery that FES is

involved in the phagocytic uptake of bacteria by neutrophils (Figure 4.1, step 3). In addition, analysis of signaling pathways downstream of FES (Figure 4.1, step 4) provides insight in the molecular mechanism via which FES regulates reorganization of the actin cytoskeleton required for receptor internalization.

Results

WEL028 reduces phagocytic uptake of bacteria by FES^{S700C} HL-60 neutrophils

HL-60 cells have been widely used to study neutrophil biology as an experimentally tractable alternative for primary neutrophils, which have a short life-span and cannot be grown in culture.[7] It was first confirmed that FES^{S700C} HL-60 cells could be differentiated into functional neutrophils. After stimulation with all-*trans*-retinoic acid (ATRA; 1 µM) and dimethylsulfoxide (DMSO; 1.25%) for 72 h, cells displayed a reduction in cell proliferation and an increase in surface expression of the neutrophil marker CD11b (Supplementary Figure 4.1A, B). Moreover, cells acquired the ability to induce an oxidative burst upon stimulation with phorbol 12-myristate 13-acetate (PMA), which is indicative for functional neutrophils (Supplementary Figure 4.1C, D).

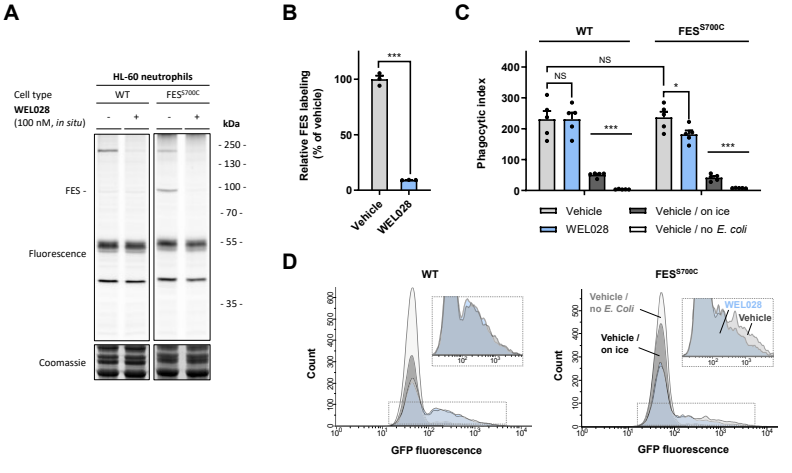

Figure 4.2 - FES inhibition reduces phagocytic uptake of *E. coli* by HL-60 neutrophils. (A, B) Complete FES inhibition at 100 nM WEL028 in FES^{S700C} HL-60 neutrophils *in situ*. Neutrophils were treated with WEL028 (100 nM, 1 h, 37 °C) and lysates were post-labeled (1 µM WEL033, 30 min, rt). Band intensities were normalized to vehicle-treated control (N = 3). **(C, D)** WEL028 reduces phagocytic uptake in FES^{S700C} but not WT neutrophils. HL-60 neutrophils were incubated with vehicle or WEL028 (100 nM, 1 h, 37 °C), after which GFP-expressing *E. coli* B834 were added (MOI = 30, 1 h, 37 °C). Cells were analyzed by flow cytometry (N = 5). Phagocytic index was calculated as fraction of GFP-positive cells (number of phagocytic cells) multiplied by GFP mean fluorescence intensity (number of phagocytized bacteria). All data represent means ± SEM. Statistical analysis was performed using ANOVA with Holm-Sidak's multiple comparisons correction, *** P <0.001; * P <0.05; NS if P >0.05.

To measure the phagocytic uptake by HL-60 neutrophils, a flow cytometry-based assay with live GFP-expressing *E. coli* was set up.[8] Control cells incubated on ice were included to account for surface binding without internalization. Both wild-type (WT) and FES^{S700C} neutrophils effectively internalized bacteria with identical phagocytic indices (Figure 4.2C), which is in line with the results from chapter 3 that indicated that wild-type and FES^{S700C} HL-60 cells behave identically. Phagocytic uptake showed a time-dependent increase up to 60 min and maximum uptake was observed at a multiplicity of infection (MOI) of 30 (Supplementary Figure 4.2). Interestingly, WEL028 (100 nM), at a concentration sufficient for complete and selective FES inactivation (Figure 4.2A, B), reduced the phagocytic index by 30-50% in FES^{S700C} expressing cells, but not in WT HL-60 neutrophils (Figure 4.2C, D). Reduced phagocytosis upon FES inhibition was consistently observed at various MOIs and infection times (Supplementary Figure 4.2). This indicates that FES activity plays an important role in phagocytosis of *E. coli* by neutrophils.

SYK kinase is a substrate of FES

The previously obtained substrate profile of FES (chapter 2) was examined in more detail to gain insight in the molecular mechanism of FES-mediated phagocytosis,. A peptide of the non-receptor tyrosine kinase ZAP70 was identified as a prominent FES substrate with high signal intensity. Incubation with WEL028 abolished peptide phosphorylation by FES^{S700C}, but not FES^{WT} (Figure 4.3A). Although ZAP70 is predominantly linked to immune signaling in T-cells, its close homolog SYK is ubiquitously expressed in various immune cells, including neutrophils.[9] Moreover, SYK is part of signaling pathways linked to

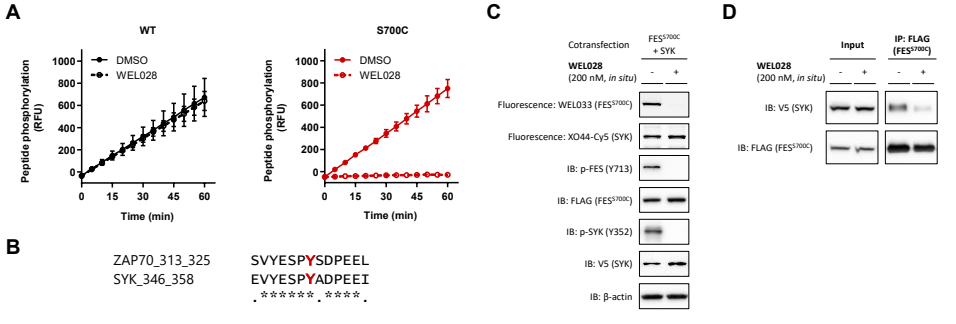

Figure 4.3 – Identification of SYK tyrosine kinase as a substrate of FES. (A) SYK Y352 as proposed phosphorylation site of FES, based on phosphorylation of homologous ZAP70 peptide by recombinant FES^{WT} (left) and FES^{S700C} (right). WEL028 selectively abolishes peptide phosphorylation by FES^{S700C} (PamChip® microarray, N = 3). **(B)** ZAP70 peptide sequence used in microarray and its homology to corresponding SYK peptide. Putative target tyrosine phosphorylation site is indicated in red. **(C)** FES phosphorylates SYK Y352 in co-transfected U2OS cells. U2OS cells co-expressing FLAG-tagged FES^{S700C} and V5-tagged SYK were incubated with vehicle or WEL028 (200 nM, 1 h, 37 °C) and lysed. Lysates were labeled (250 nM WEL033, 30 min, rt) and analyzed by in-gel fluorescence and immunoblot (N = 3). **(D)** SYK interacts with FES and this interaction is dependent on FES activity. Co-transfected U2OS cells were incubated as in C, followed by immunoprecipitation using anti-FLAG antibody and immunoblot analysis (N = 3). All data represent means ± SEM.

pathogen recognition and involved in bacterial uptake by neutrophils.[10] The identified ZAP70 peptide substrate shows high sequence similarity to its SYK counterpart surrounding Y352 (Figure 4.3B).

To validate that SYK is a downstream target of FES, SYK-V5 and FES^{S700C}-FLAG were co-transfected in U2OS cells. First, it was confirmed that overexpression of FES^{S700C} led to autophosphorylation of FES at Y713, which was sensitive to WEL028 (Figure 4.3C). Subsequent immunoblot analysis using a SYK Y352 phospho-specific antibody showed that SYK was phosphorylated in a WEL028-dependent manner. Labeling of SYK by active site lysine-targeting probe XO44-Cy5[11] was unaffected by pre-incubation with WEL028, indicating that WEL028 does not inhibit SYK directly. In addition, WEL028 did not inhibit SYK in the kinome selectivity screen (chapter 2) and did not affect SYK pY352 levels when FES^{S700C} was omitted (Supplementary Figure 4.3). Immunoprecipitation against FES^{S700C} using an anti-FLAG antibody revealed a physical interaction between FES and SYK as witnessed by immunoblot against the V5-tag of SYK (Figure 4.3D). Interestingly, this interaction was dependent on the activation status of FES, because WEL028 inhibited the co-precipitation of SYK with FES. Taken together, these results suggest that SYK Y352 is a direct substrate of FES.

FES transiently phosphorylates SYK Y352 in HL-60 neutrophils exposed to *E. coli*

Next, HL-60 neutrophils were incubated with the potent SYK inhibitor R406 to verify that endogenous SYK is also involved in phagocytic uptake of *E. coli* by neutrophils. SYK inhibition reduced phagocytosis to similar levels as observed for WEL028 (Figure 4.4A).

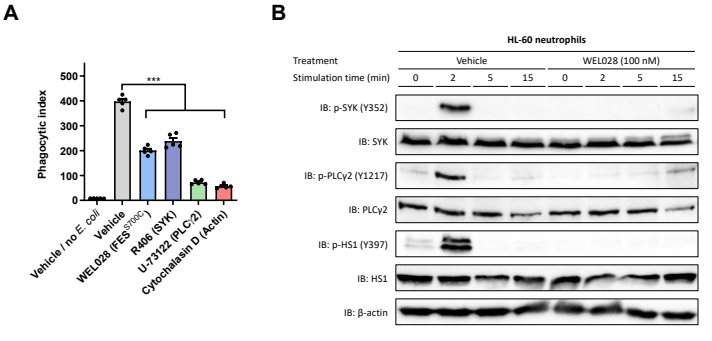

Figure 4.4 – FES phosphorylates SYK Y352 and downstream targets HS1 and PLCγ2 in HL-60 neutrophils infected with *E. coli*. (A) Phagocytic uptake of *E. coli* by HL-60 neutrophils is dependent on FES, SYK and PLCγ2 activity and requires actin polymerization. HL-60 neutrophils were incubated with vehicle or indicated compounds (100 nM WEL028, 1 µM R406, 5 µM U-73122 or 10 µM Cytochalasin D, 1 h, 37 °C), after which GFP-expressing *E. coli* B834 were added (MOI = 30, 1 h, 37°C). Cells were analyzed by flow cytometry (N = 5). **(B)** FES rapidly phosphorylates endogenous SYK Y352 and downstream substrates HS1 Y397 and PLCγ2 Y1217 in HL-60 neutrophils infected with *E. coli*. Inhibitor incubation as in A, followed by addition of GFP-expressing *E. coli* B834 (MOI = 30, 0-2-5-15 min, 37 °C) and immunoblot analysis (N = 3). All data represent means ± SEM. Statistical analysis was performed using ANOVA with Holm-Sidak's multiple comparisons correction, *** P <0.001.

Of note, phospholipase C gamma 2 (PLCγ2) inhibitor U-73122 and actin polymerization inhibitor Cytochalasin D were taken along as positive controls to verify that the phagocytosis was mediated via PLCγ2 and was actin polymerization-dependent.[2] Finally, it was investigated whether the signaling pathway downstream of SYK was modulated in a FES-dependent manner by using immunoblot analysis with phospho-specific antibodies for SYK Y352, hematopoietic cell-specific protein-1 (HS1) Y397 (an actin-binding protein) and PLCγ2 Y1217 (Figure 4.4B). Indeed, a transient phosphorylation of SYK, HS1 and PLCγ2 was observed, which peaked at 2 min after incubation with bacteria. Inhibition of FES^{S700C} completely blocked the phosphorylation of these proteins, thereby demonstrating FES activation is an early event in the phagocytosis of *E. coli* in HL-60 neutrophils.

Discussion and conclusion

In this chapter, chemical genetic tools were used to uncover a novel biological role for FES in phagocytosis by neutrophils. It was demonstrated that FES plays a key role in the phagocytic uptake of bacteria in neutrophils by activating SYK and downstream substrates HS1 and PLCγ2. In combination with previous data reported in the literature (reviewed in reference 12), these new insights led to a proposed mechanistic model for the role of FES in neutrophil phagocytosis (Figure 4.5). One of the first events in response to bacterial recognition by neutrophil surface receptors is the formation of the lipid phosphatidylinositol 4,5-bisphosphate (PIP_2) in the membrane (Figure 4.5, panel 1). FES normally resides in the cytosol in an inactive conformation. Its N-terminal F-BAR domain, a unique structural feature of FES, exclusively binds to phosphoinositide-rich lipids, such as PIP_2[6], and drives FES translocation to the membrane. This triggers the formation of oligomers and auto-activation of FES by phosphorylation on Y713 and induces membrane curvature[13,14] required for particle internalization.[6] (Figure 4.5, panel 2).

FES subsequently activates SYK by phosphorylation of Y352, which poses an alternative activation mechanism of SYK compared to the traditional activation via binding to ITAM domains of immunoreceptors.[15] Y352 is located in a linker region of SYK, which separates its two N-terminal SH2 domains from its C-terminal catalytic domain. Phosphorylation of this linker residue was previously shown to perturb auto-inhibitory interactions, resulting in SYK activation.[15] SYK is known to phosphorylate HS1, an actin-binding protein involved in reorganization of the actin cytoskeleton. HS1 can be phosphorylated on multiple tyrosine residues that all contribute to its actin remodeling function.[16] Of note, its Y378 and Y397 residues are phosphorylated by FES in mast cells, but both sites have also been identified as substrate sites for other kinases, including SYK.[6] Phosphorylation of HS1 by FES and/or SYK drives reorganization of the actin cytoskeleton required for internalization of the bacterium-receptor complex (Figure 4.5, panel 3). Concomitantly, the phosphorylated Y352 residue in SYK can serve as binding site for the SH2 domain of PLCγ2, followed by SYK-mediated PLCγ2 activation. In turn, this allows

degradation of PIP_2 into diacylglycerol (DAG) and inositoltriphosphate (IP_3), which alters the membrane composition and returns it to the non-activated state: FES dissociates from the membrane and the signaling process is terminated (Figure 4.5, panel 4).

This model thus proposes a feedback mechanism in which FES indirectly regulates its own localization and activation by modulating PLCγ2 activity via SYK. Based on the rapid, transient phosphorylation of SYK Y352 and downstream substrates (Figure 4.5B), FES seems to be rapidly deactivated, possibly via the action of phosphatases. Examination of the SH2 binding profile of FES (chapter 2) identified the phosphatases PTN6 and PTN11 as potential interaction partners of FES, but further studies are required to gain insight in the deactivation of signaling pathways underlying FES-mediated phagocytosis.

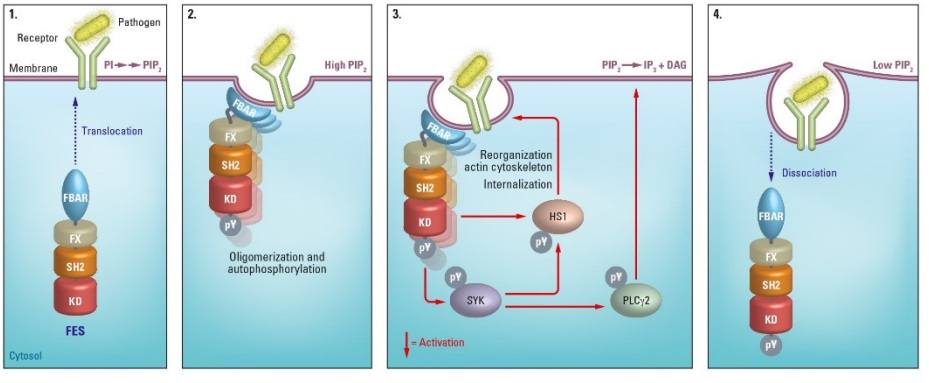

Figure 4.5 – Proposed simplified model for the role of FES in neutrophil phagocytosis. Phosphorylation sites Y378 and Y397 on HS1 are shown as a single site for visualization purposes. For detailed explanation of the model, see main text. PI: phosphatidylinositol, PIP_2: phosphatidylinositol 4,5-bisphosphate, IP_3: inositol 1,4,5-trisphosphate, DAG: diacylglycerol, FX: F-BAR extension, SH2: Src Homology 2, KD: kinase domain, pY: phosphotyrosine.

It should be noted that FES possesses an F-BAR extension (FX) domain that binds phosphatidic acid (PA) and activates its kinase activity.[17] PA is synthesized by phospholipase D (PLD) in response to activation of various immune receptors. PLD activation also leads to elevated intracellular Ca^{2+} levels, but the exact mechanistic pathways underlying this event remain poorly understood.[18] FES could possibly be a molecular link that activates PLCγ2 to increase Ca^{2+} in response to PA production by PLD. Further studies are required to investigate the activation mechanism of FES by PA and the role of FES in the complex cross-talk between PLD and PLCγ2.

Since FES is also linked to other cellular processes driven by actin reorganization, such as cell migration[19,20], it will be interesting to investigate whether FES also mediates this function in a SYK-dependent manner. Moreover, identification of FES as a potential activator of SYK may provide new insights in previous studies reporting on FES and/or SYK function. For example, FES is involved in the development and function of osteoclasts, multinucleated cells responsible for bone resorption.[21] Accordingly, SYK-deficient osteoclasts exhibit major defects in the actin cytoskeleton, resulting in reduced bone

resorption.[22] It remains to be determined whether FES inhibition disrupts the osteoclast cytoskeleton in a similar manner, which would make FES a potential target to treat osteoporosis and cancer-associated bone disease. Furthermore, FES inhibition was shown to suppress growth of acute myeloid leukemia (AML) cells that harbor an internal tandem duplication in the *FLT3* gene (*FLT3*-ITD), but not AML cells expressing wild-type FLT3.[23,24] Similarly, FLT3-ITD AML is more vulnerable to SYK suppression than FLT3-WT AML.[25] It would be interesting to investigate whether FES activates SYK in these AML cells and whether altered internalization of FLT3-ITD compared to FLT3-WT perhaps explains the increased susceptibility to FES and SYK inhibition.

Two SYK inhibitors have recently been approved by the FDA and several more are currently in clinical trials for the treatment of various malignancies and inflammatory diseases.[26] The question thus rises in what other cell types and cellular processes SYK activation is dependent on FES. Notably, FES is expressed in many cell types that contribute to the pathogenesis of inflammatory diseases, such as macrophages, mast cells, neutrophils and B-cells, but future studies will prove whether FES inhibitors may be of therapeutic value in these disorders. The chemical genetic strategy presented here may provide valuable tools to investigate FES-associated physiological processes and aid in its validation as drug target.

Acknowledgments

Riet Hilhorst, Tim van den Hooven and Rob Ruijtenbeek are kindly acknowledged for microarray measurements and helpful discussions, Daphne van Elsland for generation of the fluorescent *E. coli* strain, Laura de Paus for synthesis of XO44-Cy5, and Robert van Sluis for graphic illustrations.

Experimental procedures

General

All chemicals were purchased at Sigma Aldrich, unless stated otherwise. Cloning reagents were from Thermo Fisher. Cytochalasin D and U-73122 were purchased at Focus Biomolecules and R406 at Selleckchem. XO44-Cy5 was previously synthesized in-house according to literature procedures[11] and characterized by NMR and LC-MS. All cell culture disposables were obtained from Sarstedt.

Cloning

Full-length human cDNA encoding FES was obtained from Source Bioscience. pDONR223-construct with full-length human cDNA of SYK was a gift from William Hahn & David Root (Addgene Human Kinase ORF Collection). Eukaryotic expression construct of FES was generated by PCR amplification and restriction/ligation cloning into a pcDNA3.1 vector, in frame with a C-terminal FLAG-tag. Eukaryotic expression construct of SYK was generated using Gateway™ recombinational cloning into a pcDest40 vector, in frame with a C-terminal V5-tag, according to recommended procedures (Thermo Fisher). All plasmids were isolated from transformed XL10-Gold competent cells (prepared using *E. coli* transformation buffer set; Zymo Research) using plasmid isolation kits following the supplier's protocol (Qiagen). All sequences were verified by Sanger sequencing (Macrogen).

PamChip® microarray assay

Kinase activity assay

Kinase activity profiles were determined using the PamChip® 12 protein tyrosine (PTK) peptide microarray system (PamGene International B.V.) according to the instructions of the manufacturer, essentially as described[27] with the exception that arrays were blocked with 2% BSA and the assay buffer contained EDTA instead of EGTA. Sample input was 0.25 ng purified FES (wild-type or S700C) per array and [ATP] = 400 µM. For arrays with inhibitor, recombinant FES was pre-incubated in assay mix without ATP with vehicle or WEL028 (100 nM, 30 min, on ice, 2% final DMSO concentration).

Data analysis and quality control

Data quantification of the images at all exposure times and reaction times and visualization of the data were performed using BioNavigator software (PamGene International B.V.). Post-wash signals (local background subtracted) were used. After signal quantification and integration of exposure times, signals were log2-transformed for visualization. Peptides without ATP-dependent signal were excluded from analysis. Identification of peptides that were significantly different between conditions was performed using a Mixed Model statistical analysis.

Cell culture

General cell culture

Cell lines were purchased at ATCC and were tested on regular basis for mycoplasma contamination. Cultures were discarded after 2-3 months of use. U2OS (human osteosarcoma) cells were cultured at 37 °C under 7% CO_2 in DMEM containing phenol red, stable glutamine, 10% (v/v) high iron newborn calf serum (Seradigm), penicillin and streptomycin (200 µg/mL each; Duchefa). Medium was refreshed every 2-3 days and cells were passaged two times a week at 80-90% confluence. HL-60 (human promyeloblast) cells were cultured at 37 °C under 5% CO_2 in HEPES-supplemented RPMI containing phenol red, stable glutamine, 10% (v/v) fetal calf serum (Biowest), penicillin and streptomycin (200 µg/mL each), unless stated otherwise. Cell density was maintained between 0.2 x 10^6 and 2.0 x 10^6 cells/mL. Cell viability was assessed by Trypan Blue exclusion and quantification using a TC20™ Automated Cell Counter (Bio-Rad).

Transfection

One day prior to transfection, U2OS cells were transferred from confluent 10 cm dishes to 15 cm dishes. Before transfection, medium was refreshed (13 mL). A 3:1 (m/m) mixture of polyethyleneimine (PEI; 60 µg/dish) and plasmid DNA (20 µg/dish; for co-transfections 10 µg each) was prepared in serum-free medium and incubated for 15 min at rt. The mixture was then added dropwisely to the cells, after which the cells were grown to confluence in 48 h. Cells were then harvested by scraping in lysis buffer and lysates were prepared as described.

Differentiation of HL-60 cells

One day prior to induction of differentiation, cells were diluted to 0.4 x 10^6 cells/mL. Neutrophil differentiation was induced by addition of all-*trans*-retinoic acid (ATRA; 1 µM) and dimethylsulfoxide (DMSO; 1.25%) for 72 – 96 h.

Inhibitor treatment in live cells

The term *in situ* is used to designate experiments in which live cell cultures are treated with inhibitor, whereas the term *in vitro* refers to experiments in which the inhibitor is incubated with cell lysates. Compounds were diluted in growth medium from a 1000x concentrated stock solution in DMSO.

For *in situ* assays on live transfected cells, cells were transfected prior to treatment as described above. After 48 h, cells were treated with compound for 1 h. Cells were then harvested by scraping in lysis buffer and lysates were prepared as described.

For *in situ* treatment post-differentiation, HL-60 cells were differentiated as described above and incubated with compound for 1 h unless specified otherwise. Cells were centrifuged (200 *g*, 5 min, rt) and washed in equal volume of PBS (1000 *g*, 5 min, rt). Cell pellets were flash-frozen in liquid nitrogen and stored at -80 °C until use.

CD11b expression analysis by flow cytometry

Cells (1 x 10^6 per sample) were centrifuged (500 *g*, 3 min) and suspended in human FcR blocking solution (Miltenyi Biotec, 25x diluted in FACS buffer (1% BSA, 1% FCS, 0.1% NaN_3, 2 mM EDTA in PBS)), transferred to a V-bottom 96-well plate and incubated for 10 min at 4°C. Next, monoclonal rat CD11b-APC antibody (1:100, Miltenyi Biotec, 130-113-231) or rat anti-IgG2b-APC isotype control antibody (1:100, Miltenyi Biotec, 130-106-728) was added along with 7-aminoactinomycin D (7-AAD) (1 µg/mL) and samples were incubated for 30 min 4°C in the dark. Samples were washed once in PBS and fixed in 1% paraformaldehyde (PFA) in PBS for 15 min at 4°C in the dark, followed by two washing steps in PBS and resuspension in FACS buffer to a density of approximately 500 cells/µL. Cell suspensions were measured on a Guava easyCyte HT and data was processed using GuavaSoft InCyte 3.3 (Merck Millipore). Events (10,000 per condition) were gated by forward and side scatter (cells), side scatter area (singlets) and viability (live cells) and the percentage of CD11b-positive cells was determined based on background fluorescence for isotype control antibody and non-differentiated cells. The RED-R channel (661/15 filter) and RED-B channel (695/50 filter) were used to detect CD11b-APC and 7-AAD, respectively.

Neutrophil oxidative burst assay

Cells were centrifuged (500 *g*, 3 min), suspended in PBS and seeded in triplicate per condition in 96-well plates (100,000 cells per well in 100 µL). To each well, 100 µL of PBS containing nitroblue tetrazolium (NBT) with vehicle or phorbol 12-myristate 13-acetate (PMA) was added, bringing final concentrations to 0.1% and 1.6 µM, respectively. Cells were incubated (1 h, 37 °C) and plates were imaged by phase contrast microscopy (20x magnification, EVOS FL Auto 2). Cells positive for formazan deposits were counted (3 different fields per replicate).

Preparation of cell lysates for gel and immunoblot analysis

HL-60 cells were suspended in M-PER lysis buffer supplemented with 1x Halt™ phosphatase and protease inhibitor cocktail (Thermo Fisher). U2OS cells were directly scraped in lysis buffer and collected in tubes. Lysates were centrifuged (14,000 *g*, 10 min, 4 °C) to yield the clear lysate as supernatant. Protein concentration was determined using Quick Start™ Bradford Protein Assay (Bio-Rad) and diluted to appropriate concentration in M-PER. Lysates were aliquoted, flash-frozen and stored at -80 °C until use.

Probe labeling experiments

In situ treated cell lysate (14.5 µL) was incubated with WEL033 or XO44-Cy5 (0.5 µL, 30 x concentrated stock in DMSO, 30 min, rt). Final concentrations of inhibitors and/or probe are indicated in the main text and figure legends. Reactions were quenched with 4x Laemmli buffer (5 µL, final concentrations 60 mM Tris pH 6.8, 2% (w/v) SDS, 10% (v/v) glycerol, 5% (v/v) β-mercaptoethanol, 0.01% (v/v) bromophenol blue) and boiled for 5 min at 95°C. Samples were resolved by SDS-PAGE on a 10% polyacrylamide gel (180 V, 75 min). Gels were scanned using Cy3 and Cy5 multichannel settings (605/50 and 695/55 filters, respectively; ChemiDoc™ MP System, Bio-Rad). Fluorescence intensity was corrected for protein loading determined by Coomassie Brilliant Blue R-250 staining and quantified with Image Lab (Bio-Rad). IC_{50} curves were fitted with Graphpad Prism® 7 (Graphpad Software Inc.).

Immunoblot

Samples were resolved by SDS-PAGE as described above, but transferred to 0.2 µm polyvinylidene difluoride membranes by Trans-Blot Turbo™ Transfer system (Bio-Rad) directly after fluorescence scanning. Membranes were washed with TBS (50 mM Tris pH 7.5, 150 mM NaCl) and blocked with 5% milk in TBS-T (50 mM Tris pH 7.5, 150 mM NaCl, 0.05% Tween-20) for 1 h at rt.

Membranes were then either incubated with primary antibody in 5% milk in TBS-T (FLAG, V5, β-actin; o/n at 4 °C) or washed three times with TBS-T, followed by incubation with primary antibody in 5% BSA in TBS-T (other antibodies, o/n at 4 °C). Membranes were washed three times with TBS-T, incubated with matching secondary antibody in 5% milk in TBS-T (1:5000, 1 h at rt) and then washed three times with TBS-T and once with TBS. Luminol development solution (10 mL of 1.4 mM luminol in 100 mM Tris pH 8.8 + 100 µL of 6.7 mM *p*-coumaric acid in DMSO + 3 µL of 30% (v/v) H_2O_2) or Clarity Max™ ECL Substrate (Bio-Rad) was added and chemiluminescence was detected on ChemiDoc™ MP System.

Following detection of phospho-proteins, membranes were stripped (Restore™ Plus Stripping Buffer, Thermo Fisher) for 20 min, washed three times with TBS, and blocked and incubated with the control antibodies as described above.

Primary antibodies: monoclonal mouse anti-FLAG M2 (1:5000, Sigma Aldrich, F3156), monoclonal anti-V5 (1:5000, Thermo Fisher, R960-25), monoclonal mouse anti-β-actin (1:1000, Abcam, ab8227), polyclonal rabbit anti-phospho-FES Y713 (1:1000, Thermo Fisher, PA5-64504), polyclonal rabbit anti-phospho-SYK Y352 (1:1000, Cell Signaling Technology (CST), #2701), monoclonal rabbit anti-SYK (1:1000, CST, #13198), polyclonal rabbit anti-phospho-HS1 Y397 (1:1000, CST, #4507), polyclonal rabbit anti-HS1 (1:1000, CST, #4503), polyclonal rabbit anti-phospho-PLCγ2 Y1217 (1:1000, CST, #3871), polyclonal rabbit anti-PLCγ2 (1:1000, CST, #3872). Secondary antibodies: goat anti-mouse-HRP (1:5000, Santa Cruz, sc-2005), goat anti-rabbit-HRP (1:5000, Santa Cruz, sc-2030).

Co-immunoprecipitation

U2OS cells were co-transfected with FLAG-tagged FES and V5-tagged SYK and grown for 48 h as described above, followed by incubation with vehicle or WEL028 (200 nM) for 1 h. Cells were then washed with PBS and collected by scraping in IP-buffer (20 mM Tris-HCl pH 7.5, 150 mM NaCl, 1% Triton X-100 supplemented with 1x Halt™ phosphatase and protease inhibitor cocktail (Thermo

Fisher)). Cells were lysed by sonication on ice (3 cycles of 10 s on, 10 s off at 25% maximum amplitude), centrifuged (14,000 *g*, 10 min, 4 °C). The clear lysate was diluted to 1 mg/mL in IP-buffer and subjected to immunoprecipitation using Dynabeads™ Protein G Immunoprecipitation kit (Thermo Fisher) following manufacturer's protocol. Briefly, anti-FLAG M2 antibody (1:100, Sigma Aldrich, F3156) was incubated with beads with gentle rotation (10 min, rt), after which lysate (500 µL of 1 mg/mL) was added and incubated (1 h, 4 °C). Beads were washed three times, transferred to clean tubes and eluted by suspension in 2x Laemmli buffer (50 µL, 10 min, 70 °C). Samples (10 µL per lane) were resolved by SDS-PAGE and immunoblotted using anti-V5 or anti-FLAG antibodies. Immunoprecipitations were performed in three independent replicates.

Phagocytosis assays

Flow cytometry

HL-60 cells were differentiated to neutrophils as described. Cells were counted and centrifuged (200 *g*, 5 min), followed by resuspension in growth medium without antibiotics. Cells were incubated with vehicle or inhibitor (from 1000x concentrated stocks in DMSO) for 1 h at 37°C prior to infection (1 x 10^6 cells in 900 µL in 12-well plate). Meanwhile, *E. coli* B834(DE3) constitutively expressing GFP^{A206K} were grown in LB medium to an OD600 of 0.4-1.0, after which bacteria were centrifuged (2,000 *g*, 5 min), washed and resuspended in PBS to appropriate density.[8] Neutrophils were infected by addition of bacteria at multiplicity of infection (MOI) of 30 unless stated otherwise. Cells were then incubated for 1 h at 37°C unless stated otherwise, after which cells were resuspended and transferred to Eppendorf tubes, washed in FACS buffer (1% BSA, 1% FCS, 0.1% NaN_3, 2 mM EDTA in PBS; 1 mL, 500 *g*, 3 min) and fixed in 1% paraformaldehyde (PFA) in PBS (15 min, 4 °C, in the dark). Fixed cells were washed twice in PBS and resuspended in FACS buffer to a density of approximately 500 cells/µL.

Cell suspensions were measured on a Guava easyCyte HT and data was processed using GuavaSoft InCyte 3.3 (Merck Millipore). Events (20,000 per condition) were gated by forward and side scatter (cells), side scatter area (singlets) and the percentage of GFP-positive cells and GFP mean fluorescence intensity (MFI) were determined based on background fluorescence for non-infected cells. The GREEN-B channel (525/30 filter) was used to detect GFP. Phagocytic index was calculated as fraction of GFP-positive cells (number of phagocytic cells) multiplied by GFP MFI (number of phagocytized bacteria).

Stimulation for detection of phosphoproteins

HL-60 neutrophils were infected as described above, but in 15 mL tubes (5 x 10^6 cells in 4 mL per sample). After indicated infection times, ice-cold PBS was added (10 mL) and suspensions were immediately centrifuged (3,500 *g*, 2 min). Supernatant was completely aspirated and cells were thoroughly resuspended in 2x Laemmli sample buffer (100 µL), followed by incubation at 95 °C for 10 min and brief sonication to reduce sample viscosity. Samples were stored at -20 °C or immediately resolved by SDS-PAGE (20 µL per lane).

Statistical analysis

All statistical measures and methods are included in the respective Figure or Table captions. In brief: all replicates represent biological replicates and all data represent means ± SEM, unless indicated otherwise. Statistical significance was determined using Student's *t*-tests (two-tailed, unpaired) or ANOVA with Holm-Sidak's multiple comparisons correction. *** $P < 0.001$; ** $P < 0.01$; * $P < 0.05$; NS if $P > 0.05$. All statistical analyses were conducted using GraphPad Prism® 7 or Microsoft Excel.

Supplementary Data

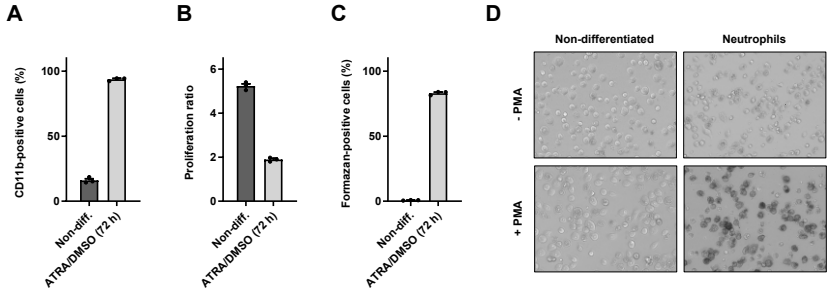

Supplementary Figure 4.1 – FES^{S700C} HL-60 cells differentiate into functional neutrophils. (A) CD11b surface expression analyzed by flow cytometry. Differentiation was induced by addition of ATRA (1 µM) and DMSO (1.25%) for 72 h. Threshold for CD11b-positive cells was determined using isotype control antibody. **(B)** Proliferation of FES^{S700C} HL-60 cells subjected to neutrophil differentiation. Proliferation ratio: live cell number after differentiation divided by live cell number before differentiation. **(C, D)** Ability of FES^{S700C} HL-60 neutrophils to induce oxidative burst upon PMA stimulation. Cells were incubated with 0.1% NBT with or without PMA (1.6 µM, 1 h, 37 °C), imaged by phase contrast microscopy (20x magnification) and cells positive for formazan deposits were counted. Data represent means ± SEM (N = 3, with 9 different fields per replicate for C, D).

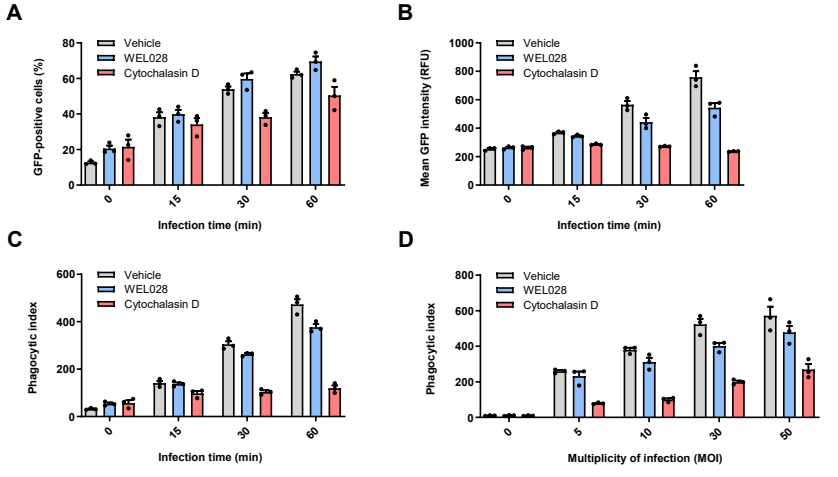

Supplementary Figure 4.2 - Phagocytic uptake of *E. coli* by HL-60 FES^{S700C} neutrophils at variable multiplicity of infection (MOI) and infection time. (A-C) HL-60 FES^{S700C} neutrophils were incubated with vehicle, WEL028 (100 nM) or Cytochalasin D (10 µM) for 1 h, after which GFP-expressing *E. coli* were added at MOI of 30. After indicated times, cells were washed and fixed (1% PFA, 15 min, 4 °C), followed by flow cytometry analysis. Phagocytic index (C) was calculated as fraction of GFP-positive cells (number of phagocytic cells, A) multiplied by GFP MFI (number of phagocytized bacteria, B). **(D)** Neutrophils were treated as in panel A-C, but with a variable MOI for 1 h. Data represent means ± SEM (N = 3).

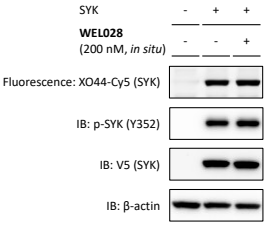

Supplementary Figure 4.3 - WEL028 does not affect SYK Y352 phosphorylation in U2OS cells in absence of FES^{S700C}. U2OS cells were transfected with only V5-tagged SYK. After 48 h, cells were incubated with vehicle or WEL028 (200 nM, 1 h) and lysed. Lysates were incubated with WEL033 (250 nM, 30 min, rt) and analyzed by in-gel fluorescence and immunoblot (N = 3).

References

1. Kumar, H., Kawai, T. & Akira, S. Pathogen recognition by the innate immune system. *Int. Rev. Immunol.* **30**, 16–34 (2011).
2. Rosales, C. & Uribe-Querol, E. Phagocytosis: A Fundamental Process in Immunity. *BioMed Research International* **2017**, 1–18 (2017).
3. Teng, T. S., Ji, A. L., Ji, X. Y. & Li, Y. Z. Neutrophils and immunity: From bactericidal action to being conquered. *Journal of Immunology Research* **2017**, 1–14 (2017).
4. Zirngibl, R. A., Senis, Y. & Greer, P. A. Enhanced Endotoxin Sensitivity in Fps/Fes-Null Mice with Minimal Defects in Hematopoietic Homeostasis. *Mol. Cell. Biol.* **22**, 2472–2486 (2002).
5. Kim, J. & Feldman, R. A. Activated Fes protein tyrosine kinase induces terminal macrophage differentiation of myeloid progenitors (U937 cells) and activation of the transcription factor PU.1. *Mol. Cell. Biol.* **22**, 1903–18 (2002).
6. McPherson, V. A. *et al.* Contributions of F-BAR and SH2 Domains of Fes Protein Tyrosine Kinase for Coupling to the Fc RI Pathway in Mast Cells. *Mol. Cell. Biol.* **29**, 389–401 (2009).
7. Hauert, A. B., Martinelli, S., Marone, C. & Niggli, V. Differentiated HL-60 cells are a valid model system for the analysis of human neutrophil migration and chemotaxis. *Int. J. Biochem. Cell Biol.* **34**, 838–854 (2002).
8. Van Elsland, D. M. *et al.* Detection of bioorthogonal groups by correlative light and electron microscopy allows imaging of degraded bacteria in phagocytes. *Chem. Sci.* **7**, 752–758 (2016).
9. Amulic, B., Cazalet, C., Hayes, G. L., Metzler, K. D. & Zychlinsky, A. Neutrophil Function: From Mechanisms to Disease. *Annu. Rev. Immunol.* **30**, 459–489 (2012).
10. Tohyama, Y. & Yamamura, H. Protein tyrosine kinase, Syk: A key player in phagocytic cells. *Journal of Biochemistry* **145**, 267–273 (2009).
11. Zhao, Q. *et al.* Broad-spectrum kinase profiling in live cells with lysine-targeted sulfonyl fluoride probes. *J. Am. Chem. Soc.* **139**, 680–685 (2017).
12. Craig, Andrew, W. B. FES/FER kinase signaling in hematopoietic cells and leukemias. *Front. Biosci.* **17**, 861 (2012).
13. Shimada, A. *et al.* Curved EFC/F-BAR-Domain Dimers Are Joined End to End into a Filament for Membrane Invagination in Endocytosis. *Cell* **129**, 761–772 (2007).
14. Carman, P. J. & Dominguez, R. BAR domain proteins—a linkage between cellular membranes, signaling pathways, and the actin cytoskeleton. *Biophysical Reviews* **10**, 1587–1604 (2018).
15. Bradshaw, J. M. The Src, Syk, and Tec family kinases: Distinct types of molecular switches. *Cellular Signalling* **22**, 1175–1184 (2010).
16. Castro-Ochoa, K. F., Guerrero-Fonseca, I. M. & Schnoor, M. Hematopoietic cell-specific lyn substrate (HCLS1 or HS1): A versatile actin-binding protein in leukocytes. *Journal of Leukocyte Biology* **105**, 881–890 (2019).
17. Di Fulvio, M. *et al.* Phospholipase D2 (PLD2) shortens the time required for myeloid leukemic cell differentiation: Mechanism of action. *J. Biol. Chem.* **287**, 393–407 (2012).
18. Nunes, P. & Demaurex, N. The role of calcium signaling in phagocytosis. *J. Leukoc. Biol.* **88**, 57–68 (2010).
19. Smith, J. A., Samayawardhena, L. A. & Craig, A. W. B. Fps/Fes protein-tyrosine kinase regulates mast cell adhesion and migration downstream of Kit and β1 integrin receptors. *Cell. Signal.* **22**, 427–436 (2010).
20. Voisset, E. *et al.* FES kinase participates in KIT-ligand induced chemotaxis. *Biochem. Biophys. Res. Commun.* **393**, 174–178 (2010).
21. Hellwig, S. *et al.* Small-molecule inhibitors of the c-Fes protein-tyrosine kinase. *Chem. Biol.* **19**, 529–540 (2012).
22. Zou, W. *et al.* Syk, c-Src, the αvβ3 integrin, and ITAM immunoreceptors, in concert, regulate osteoclastic bone resorption. *J. Cell Biol.* **176**, 877–888 (2007).
23. Voisset, E. *et al.* FES kinases are required for oncogenic FLT3 signaling. *Leukemia* **24**, 721–728 (2010).
24. Weir, M. C. *et al.* Dual inhibition of Fes and Flt3 tyrosine kinases potently inhibits Flt3-ITD+ AML cell growth. *PLoS One* **12**, e0181178 (2017).
25. Puissant, A. *et al.* SYK Is a Critical Regulator of FLT3 in Acute Myeloid Leukemia. *Cancer Cell* **25**, 226–242 (2014).
26. Roskoski, R. Properties of FDA-approved small molecule protein kinase inhibitors. *Pharmacological Research* **144**, 19–50 (2019).
27. Rosenberger, A. F. N. *et al.* Protein kinase activity decreases with higher braak stages of Alzheimer's disease pathology. *J. Alzheimer's Dis.* **49**, 927–943 (2015).